sustainability

MDPI

Article

Security Analysis of Hybrid Multi-Carrier Energy Systems

Javad Estakhr, Mohsen Simab * and Taher Niknam

Department of Electrical Engineering, Marvdasht Branch, Islamic Azad University, Marvdasht, Iran; javad.estakhr@miau.ac.ir (J.E.); niknam@sutech.ac.ir (T.N.)
* Correspondence: msimab@miau.ac.ir

Abstract: Multi-carrier energy systems (MCESs) provide collaboration between various kinds of energy carriers to supply the electricity, heating, and cooling demands. With the widespread use of MCESs in recent years, the security assessment of energy systems has attracted the attention of many contemporary researchers. However, the complexity of an MCES, including electrical, natural gas, and district heating networks, and different uncertainties imposes vast challenges to keep a safe operation energy supply. In this paper, a systematic methodology for the security analysis of MCESs is presented. For this purpose, considering electrical, natural gas, and district heating networks, an integrated model of energy systems is introduced. The security analysis of this framework is evaluated using some indices. In this approach, two well-known performance indices, including power performance index (PIP) and voltage performance index (PIV), are used to analyze the electrical networks' security. Besides, the concept of Energy not supplied (ENS) is used for natural gas and district heating networks. In this regard, security analysis of a typical MCES including the IEEE 14-bus electrical network, the IEEE 30-bus electrical network, 20-node Belgian natural gas network, and 14-node district heating network is examined. The applicability of the proposed technique will be proven using comprehensive simulation analysis.

Keywords: multi-carrier energy system (MCES); security analysis; security indices; energy not supplied (ENS)

check for updates

Citation: Estakhr, J.; Simab, M.; Niknam, T. Security Analysis of Hybrid Multi-Carrier Energy Systems. *Sustainability* **2021**, *13*, 3102. https://doi.org/10.3390/su13063102

Received: 4 January 2021
Accepted: 12 February 2021
Published: 12 March 2021

Publisher's Note: MDPI stays neutral with regard to jurisdictional claims in published maps and institutional affiliations.

Copyright: © 2021 by the authors. Licensee MDPI, Basel, Switzerland. This article is an open access article distributed under the terms and conditions of the Creative Commons Attribution (CC BY) license (https://creativecommons.org/licenses/by/4.0/).

1. Introduction

This clearly implies that electricity is regarded as a particular important part across all types of energy such as heat, cold, and gas in the next-generation energy sectors. The main reasons for this fact, it can be noted (i) the significant developments in the renewable-based power generation systems (ii) increasing attention to the utilization of high-efficiency power generation systems such as heat pumps in other energy areas like heating and cooling networks [1]. Thus, in addition to the attempts to offer new efficient solutions for renewable technologies, it will be useful to implement novel methodologies for ameliorating the power output of distributed energy technologies in a cost-effective scheme [2,3].

The combined heat and power (CHP), as one of the most common distributed energy technologies, not only can generate heat and power, but also efficiency of system can be increased up to 90%. Besides, the greenhouse gas (GHG) emissions and its related threatens can be reduced by almost 13–18% [4]. Planning and operating in the presence of CHP necessitates to study the issues such as high reliability and security in the supply of energy required for more coupled systems entitled "carrier energy systems" [5–7]. The need to adopt various types of energy carriers and human needs to provide their energy requirements has also become an important reason for the emergence of these systems [8,9]. For a more practical description of these systems, the concept of energy hub has been used which combines various energy units with distinct infrastructures.

With the expansion of the above view and the need for multi-carrier energy systems (MCESs) about the role of this issue in the energy industry, the utilization of networks such as electrical, natural gas, and district heating networks is inevitable [4,10,11]. The

main reason for implementing MCESs is to study the interactions of energy networks with each other, minimizing costs and consumer supply security [12,13]. Following the concept of the energy hub in 2005, a decomposition technique was introduced by Arnold and Anderson in 2008 [14] to convert the optimal power flow (OPF) into multiple sub-problems and solve them using repetitive but coordinated methods to cover the subject. In a more comprehensive study, authors of [15] developed the multi-agent genetic algorithm for solving the multi-carrier OPF where a non-convex optimization problem without removing the main advantages of analysis MCESs is, continuously, decomposed into its conventional OPF.

Based on the load flow approach, the gas load flow problem with the consideration of compressors has been solved in [6] using the Newton-nodal scheme. However, in [16], the transmission lines of the electrical network were not considered. Therefore, in the same year, the authors extended this research with another innovation called gas load distribution, considering the consumption flows of gas generators as loads in the mentioned network. For instance, an MCES with two fixed and variable efficiency approaches has been developed in [17] for the equipment of an energy hub using heuristic methodologies to minimize the cost of energy networks. A unified framework is adopted in [18] to combine various infrastructures, including electrical, natural gas, and district heating networks, while the power flow problem has been solved by the Newton Raphson (NR) technique.

Regarding the issue of security and reliability, the authors of [19] studied the reliability assessment of MCESs with different levels of demand in various climatic conditions. To appraise the reliability of the MCES suggested in [19] under various situations, different sizes of network equipment with two distinct weather conditions are analyzed. The planning of MCESs in the presence of wind resources is investigated in [20] by considering the N-1 events related to the gas pipeline and power transmission lines. The security zone of integrated natural gas-electricity networks in a decision-making area is discussed in [21]. To evaluate the security of MCESs, this research work first introduces the concept of the security zone. The hyperplane approximation method is used to obtain the essential boundaries and further determine the security zone based on the critical points. In this regard, in [17], the gas network's security zone in the MCES concerning the impact of the integrated electrical and natural gas networks has been studied. Research on evaluating the reliability of an MCES based on the concept of energy hub [22] has been analyzed. Assessing the reliability of the MCES under the uncertainty of the natural gas pipeline network is accomplished in [23]. In this study, an analytical method that can provide a probabilistic aspect of gas network pipelines is adopted for evaluating the reliability of the integrated system. Likewise, a systematic methodology, which can offer managers with extensive knowledge of system reliability, is developed in [24] to analyze the supply reliability of an MCES under fluctuation of demand and uncertainties renewable resources. By formulating a bi-level optimization scheme, a model of the security-constrained economic dispatch has been presented in [24] for an integrated natural gas system with wind power penetration. The purpose of [25] is to analyze energy storage technologies from the perspective of energy security, while the influence of interdependency of electrical and natural gas networks in view of the security system has been discussed in [26].

This paper aims to offer a comprehensive model for security analysis of MCESs [27–29]. For this purpose, an MCES is modeled in which electrical, natural gas, and district heating networks are considered as the energy networks. The proposed model allows combining the various infrastructures of the MCES with different properties while preserves the security problem of the overall system. The model is configured in such a way that derives the right balance between the efficiency of simulation and the computational need for the security analysis. From a security perspective, this paper seeks to ensure the power system's security to maintain the system in good working order. In the event that equipment of the power system fails (for example, the generation unit is out of the circuit due to defect; or its maximum production capacity is restricted), the rest of the system in this situation can

compensate for the performance of the equipment. In conclusion, the contributions of this paper are as follows:

- The security assessment of MCESs with various energy networks, including electrical, natural gas, and district heating networks, is analyzed.
- In the electrical network, the NR technique is adopted to investigate possible events, where the calculation of the performance indices is made by employing the PIP and PIV for each line or component.
- The security assessment of natural gas and district heating networks is accomplished by adopting the concept of Energy not supplied (ENS).

Finally, the applicability of the proposed strategy on the IEEE-14 bus electrical network, the IEEE 30-bus electrical network, 20 nodes Belgian natural gas network, and 14 node district heating network is investigated. Table 1 illustrates a comparison between the suggested model and the state-of-the-art methods in the literature.

Table 1. Comparison of contributions of suggested scheme and the literature.

	Type of Energy Carriers	Technique Formulation	Energy Not-Supplied Analysis	Sensitivity Analyisis of the PIV/PIV
Proposed Model	IEEE 14-bus system, IEEE 30-bus, 20-node Belgian gas network, and 14-node district 18 heating network	Newton-Raphson (N-R)		
Ref. [5]	IEEE 14-bus electrical network, a 15-node gas network and Belgian gas network	Newton-Raphson (N-R)	*X*	
Ref. [29]	Six bus power network and 24-bus IEEE electrical network	Mixed integer linear programming (MILP)		*X*
Ref. [30]	26 bus power system	Newton-Raphson (N-R)	*X*	
Ref. [31]	Electrical and gas networks with 32 demand points	Genetic algorithm (GA)		*X*
Ref. [32]	IEEE-33 bus system with 14-node gas system combined with the IEEE 118-bus power system and Belgian gas network	Hierarchical decoupling optimization		*X*

The rest of this paper is organized as follows: Section 2 presents the models of Multi-carrier energy systems, while the security issue is formulated in Section 3. The security analysis is conducted in Section 4 by simulating a MCES, including electrical, natural gas, and thermal networks. The obtained results are concluded in Section 5.

2. MCES Modeling

2.1. Electrical Network

The constraints of the electrical network can be expressed using the following equations [18].

$$P_{E,i}^{gen} = P_{E,i}^{dem} + Re(V_i \sum_{j=1}^{N_E} Y_{ij}^* V_j^*) \quad (1)$$

$$Q_{E,i}^{gen} = Q_{E,i}^{dem} + im(V_i \sum_{j=1}^{N_E} Y_{ij}^* V_j^*) \quad (2)$$

The above equations show the active and reactive power balance in an electrical network. The second part of the above equations shows the power passing through the lines connected to bus-i.

2.2. Natural Gas Network

In summary, the Equations (3)–(5) are commonly used for the gas network [33,34].

$$f_{G,i}^{gen} = f_{G,i}^{dem} + \sum_{j=1}^{N_G} f_{G,ij}^{line} \tag{3}$$

$$sign\left(f_{G,ij}^{line}\right) f_{G,ij}^{line2} = C_{G,ij}^{line2}\left(P_{r,i}^{2} - P_{r,j}^{2}\right) \tag{4}$$

$$C_{G,ij}^{line} = \varepsilon_G \frac{18.06\ T_0\ D_{G,ij}^{line8/3}}{P_{r0}\sqrt{\delta_G L_{G,ij}^{line} T_G Z_G}} \tag{5}$$

In this work, the analysis of load distribution in the gas network was carried out using the Newton–Raphson method. In this method, two types of nodes are considered for thermal networks—nodes whose injection flow is known, but the pressure of the corresponding node is unknown. There are other nodes that, unlike the previous type, have a known pressure but an unknown injection flow, which we will follow during the load distribution process. The nodes of the second type are generally considered as reference nodes. Finally, it should be noted that in gas networks, it is assumed that no leakage occurs during gas transmission. Thus, in solving the distribution of gas loads, the goal is to find the pressure of the nodes and the amount of flow produced by the reference node. With these values, the flow rate through the pipelines is also obtained.

2.3. District Heating Network

A district heating network consists of two reciprocating circuits, as shown in Figure 1. The circuit transfers the hot water from the source to the loads. The heated water enters the return circuit after entering the thermal loads by losing its temperature. The return water returns to the heat sources and enters the transmission lines by increasing the temperature again and gaining the necessary thermal power, and the said cycle is completed. In the meantime, the purpose of heat network analysis is to find the amount of heat produced in reference sources, the amount of heat transferred from the lines, water flow, and heat losses resulting from the difference between ambient temperature and pipelines. The amount of heat transfer power between two points depends on the mass flow rate and the temperature difference between the two points [33,34].

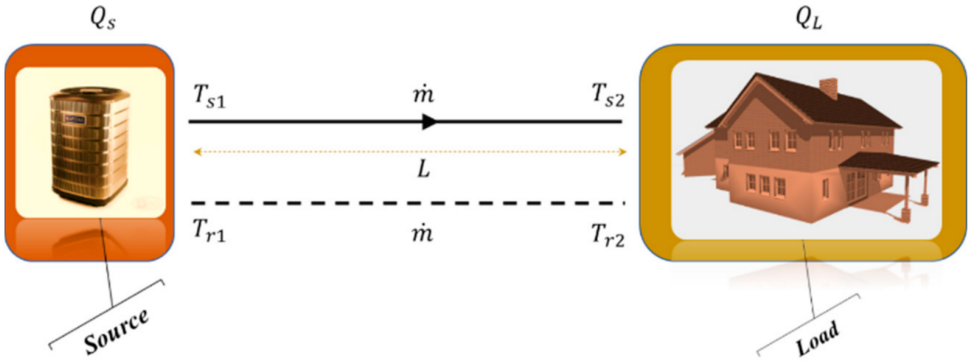


Figure 1. Heat network with a reciprocating path.

In this Figure, the upper pipeline transfers the heated water from the source to the heat load. After wasting the heated water in the path of passing and crossing the thermal load and supplying it with a certain and constant temperature (assumption of this article),

it leaves the heat load and returns to the source. In this case, the amount of heat sent by the source is obtained from the following equation.

$$Q_s = \dot{m} c_p (T_{s1} - T_{r1}) \tag{6}$$

The balance of heat power in the whole system can be expressed as follows:

$$Q_s = \dot{m} c_p (T_{s2} - T_{r2}) + \dot{m} c_p (T_{s1} - T_{s2}) + \dot{m} c_p (T_{r2} - T_{r1}) \tag{7}$$

The temperature drop in the heat pipelines can be expressed as follows:

$$T_{s,j} = \psi_{H,ij}^{line} (T_{s,i} - T_g) + T_g \tag{8}$$

$$T_{r,j} = \psi_{H,ij}^{line} (T_{r,i} - T_g) + T_g \tag{9}$$

$$\psi_{H,ij}^{line} = \exp\left(-\frac{L_{H,ij}^{line} U}{c_p \dot{m}_{H,ij}^{line}} \right) \tag{10}$$

2.4. Network Components

2.4.1. Gas Power Plants

Generator heat rate (*HR*) curves are related to the ratio of fuel consumption to power output. The mathematical expression of this problem is as follows [35]:

$$HR_i^{gen} = a_i^{gen} \left(P_{E,i}^{gen} \right)^2 + b_i^{gen} P_{E,i}^{gen} + c_i^{gen} \tag{11}$$

In addition, *HR* expresses the amount of thermal power required to produce the desired electrical power. This parameter can be used for the amount of fuel needed to create such heat power. Assuming that the fuel used by the generators is natural gas, the amount of natural gas required to generate power by this generator is obtained from (12), in which GHV_G is the amount of gross heating value.

$$f_{G,i}^{gen} = \frac{HR_i^{gen}}{GHV_G} \tag{12}$$

2.4.2. Combined Heat and Power (CHP)

Another unit of energy production that has been studied in this work is the units of simultaneous production of heat and electricity. In many countries, CHP has been added to the power grid to generate both electricity and heat.

The heat power generated at the CHP output is considered constant. Therefore, the following equation can be used to calculate the amount of electrical power by this unit [19]:

$$P_{E,i}^{chp} = \begin{cases} a_i^{chp} Q_{H,i}^{chp} + b_i^{chp} T_{s,i}^{chp} + c_i^{chp} & , d_{1,i}^{chp} Q_{H,i}^{chp} \le Q_{H,i}^{chp} \le d_{2,i}^{chp} Q_{H,i}^{chp,max} \\ a_i^{chp} Q_{H,i}^{chp} + b_i^{chp} T_{s,i}^{chp} + c_i^{chp} - y_{1,i}^{chp} & , d_{2,i}^{chp} Q_{H,i}^{chp,max} \le Q_{H,i}^{chp} \le d_{1,i}^{chp} Q_{H,i}^{chp,max} \\ a_i^{chp} Q_{H,i}^{chp} + b_i^{chp} T_{s,i}^{chp} + c_i^{chp} - y_{1,i}^{chp} - y_{2,i}^{chp} & , Q_{H,i}^{chp,min} \le Q_{H,i}^{chp} \le d_{2,i}^{chp} Q_{H,i}^{chp,max} \end{cases} \tag{13}$$

The parameters $y_{1,i}^{chp}$ and $y_{2,i}^{chp}$ are called load effect constants and are obtained from the following equations:

$$y_{1,i}^{chp} = \left(d_{1,i}^{chp} Q_{H,i}^{chp,max} - Q_{H,i}^{chp} \right) e_{1,i}^{chp} \tag{14}$$

$$y_{2,i}^{chp} = \left(d_{2,i}^{chp} Q_{H,i}^{chp,max} - Q_{H,i}^{chp} \right) e_{2,i}^{chp} \tag{15}$$

All the coefficients of (14) and (15) are fixed, and their values are given in [33]. To calculate the amount of gas consumed by these units, one can say:

$$f_{G,i}^{chp} = \frac{3.412}{GHV_G}\left(\frac{P_{E,i}^{chp} + Q_{H,i}^{chp}}{\eta_{t,i}^{chp}}\right) \tag{16}$$

It is worth mentioning that the coefficient of 3.412 has been used to match the unit and dimension of the parties to the equation, because the unit GHV_G is usually in terms of BTU/m^3 and the unit of interest for electrical power and thermal power in the expressed relations is watts. It should be noted that the amount of gas consumed, calculated from (16), will be in terms of standard cubic meters per hour (SCM /h).

2.4.3. Gas Boiler

The amount of gas required by the boiler to produce a certain amount of heat at its outlet can be obtained from the following equation [33]:

$$f_{G,i}^{boil} = \frac{3.412}{GHV_G}\left(\frac{Q_{H,i}^{boil} + a_i^{boil} Q_{H,i}^{boil,max}}{b_i^{boil}}\right) \tag{17}$$

2.4.4. Compressor

Gas networks for gas transmission over long distances face pressure-drop problems in remote locations. On the other hand, a certain amount of pressure is required to supply the consumers of the network. Compressors are used to compensate for pressure drops and control their profile. The compression ratio can be expressed as follows [36]:

$$H_{G,ij}^{comp} = \frac{Pr_{i,out}^{comp}}{Pr_{i,in}^{comp}} \tag{18}$$

The amount of energy consumed by the compressor in terms of horsepower per hour is equal to:

$$E_{ij}^{comp} = \frac{151.4653}{\eta_{ij}^{comp}} \frac{Pr_0}{T_0} \frac{\lambda_G}{\lambda_G - 1} z_G T_G f_{G,\,ij}^{line}\left(\left(H_{G,ij}^{comp}\right)^{\frac{\lambda_G - 1}{\lambda_G}} - 1\right) \tag{19}$$

The amount of electrical power that an electric compressor consumes is related to the amount of energy it consumes, as follows:

$$P_{E,i}^{comp} = \left(\frac{745.7 \times 10^{-6}}{3600}\right) E_{ij}^{comp} \tag{20}$$

2.4.5. Circulating Pump

In the heat networks, the circulating pumps are utilized for sending and pumping heated water. The amount of power required by pumps is derived from the following equation [9]:

$$P_{E,i}^{pump} = \frac{\dot{m}_{H,i}^{pump} g H^{pump}}{\eta_i^{pump}} \tag{21}$$

3. Security Indices in MCESs

3.1. Performance Index of Power (PIP)

In assessing the safety, overload lines, transformers, and other equipment, as well as overvoltage and voltage reduction in the bus will be studied. To evaluate the static security

from the point of view of overload of power system lines and equipment, the Performance Index (PI) of (22) is frequently adopted in the literature [37,38]:

$$PIP = \sum_{l=1}^{NL} \frac{w_l}{2n} \left[\frac{P_l}{P_l^{Max}} \right]^{2n} \tag{22}$$

where P_l is the power passing through the l^{the} line in terms of MW and P_l^{Max} is the maximum apparent power passing through the l^{the} line in terms of MW (thermal limit), NL is the number of power system lines, w_l is the positive weight coefficient for each line (if some network lines are more important, the weight factor for those lines can be considered larger), and n is a fixed number, where its larger values mean that the effect of overloaded lines is greater. In most studies, the values of w_l and n are generally set as 1 and 2, respectively.

3.2. Performance Index of Voltage (PIV)

One of the drawbacks of the performance indicator presented above is that this relationship only considers the overload of lines and other network equipment and does not take into account the voltage of the buses. In order to solve this problem, the efficiency index for bus voltage is usually defined as the following equation [37,39]:

$$PIV = \sum_{i=1}^{M} \frac{w_{vi}}{2n} \left[\frac{|V_i| - \left|V_i^{sp}\right|}{\Delta V_i^{lim}} \right]^{2n} \tag{23}$$

where $V_i^{sp} = \left(V_i^{Max} + V_i^{min}\right)/2$ and $\Delta V_i^{lim} = \left(V_i^{Max} - V_i^{min}\right)/2$. Here, w_{vi} is the weight factor for each of the buses. If some network buses are more important, the weight factor related to those buses can be considered larger. In addition, n is a constant number, and its larger values indicate the greater effect of the buses on the voltage, which is more or less the allowable value. V_i^{min} and V_i^{Max} are the minimum and maximum acceptable voltages on the i^{the} bus, respectively.

3.3. Energy Not Supplied (ENS)

In this paper, the Energy not supplied (ENS) is used to assess the security of natural gas and district heating networks [40,41]. This index is calculated as the amount of load lost due to the definite effect of a line or the outage of a unit. The following indicators can be used for these two networks:

$$fif_i = \frac{f_d - f_g}{f_d} * 100, \; QIQ_i = \frac{Q_d - Q_g}{Q_d} * 100 \tag{24}$$

With the output of each element of the natural gas network, fif_i is calculated. In other words, fif_i indicates the amount of gas ENS in the i^{the} event. The higher the value of this parameter, the higher the unloaded load. Higher values of this parameter also mean an increase in untimely times. It should be noted that the district heating network has two categories of return lines. In this paper, it is assumed that if one of the lanes goes out of the network, the corresponding return line is also removed. Thus, with the output of each of these elements, QIQ_i is calculated. In other words, QIQ_i indicates the amount of thermal ENS in the event i.

The proposed method solves the problem sequentially. It should be noted that the solutions of load flow of the electrical network are derived using the NR method, while the natural gas and district heating networks are solved only by calculating the ENS values. The flowchart of the proposed model is presented as depicted in Figure 2.

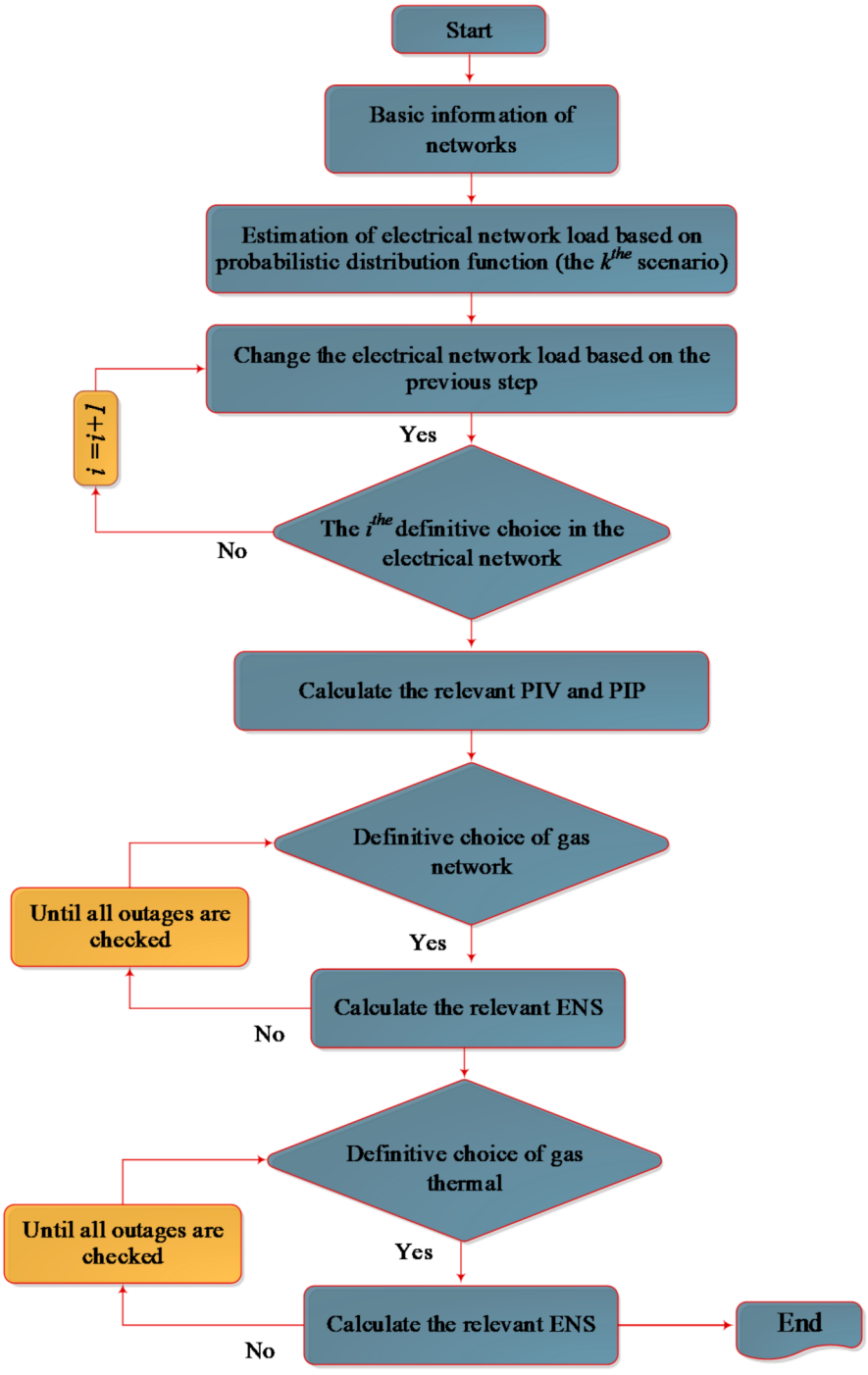


Figure 2. The flowchart of the proposed model.

4. Simulation Results

4.1. Test System

The security studies of the MCESs are carried out in the MATLAB software. Firstly, the experiments are performed in an IEEE-14 bus electrical network, which has been frequently studied in the literature [42]. In order to generalize the proposed method and use multiple networks in the simulation, in addition to the first case test, 30 electric bus networks were analyzed [34,43]. Figures 3–6 illustrate a multi-carrier system, including an IEEE 14-bus electrical network, IEEE 30-bus electrical network, 20-node Belgian natural gas network, and 14-node district heating network. In addition, the required data are listed in Table 2.

The definitions of system parameters and abbreviations are presented in nomenclature section. Connections between different devices under the networks are based on Table 3. Further details and the required data of these networks associated with each test-system are provided in [18,34,44,45].

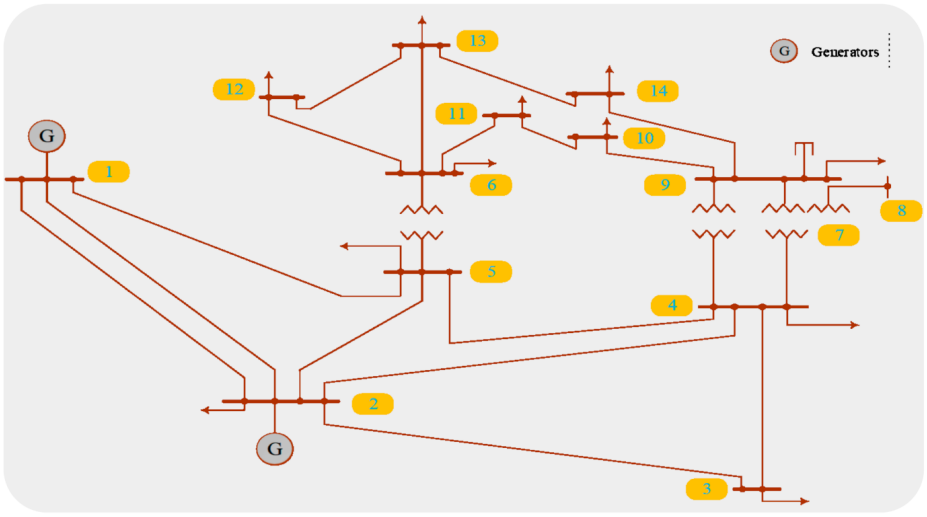


Figure 3. The IEEE 14-bus electrical network.

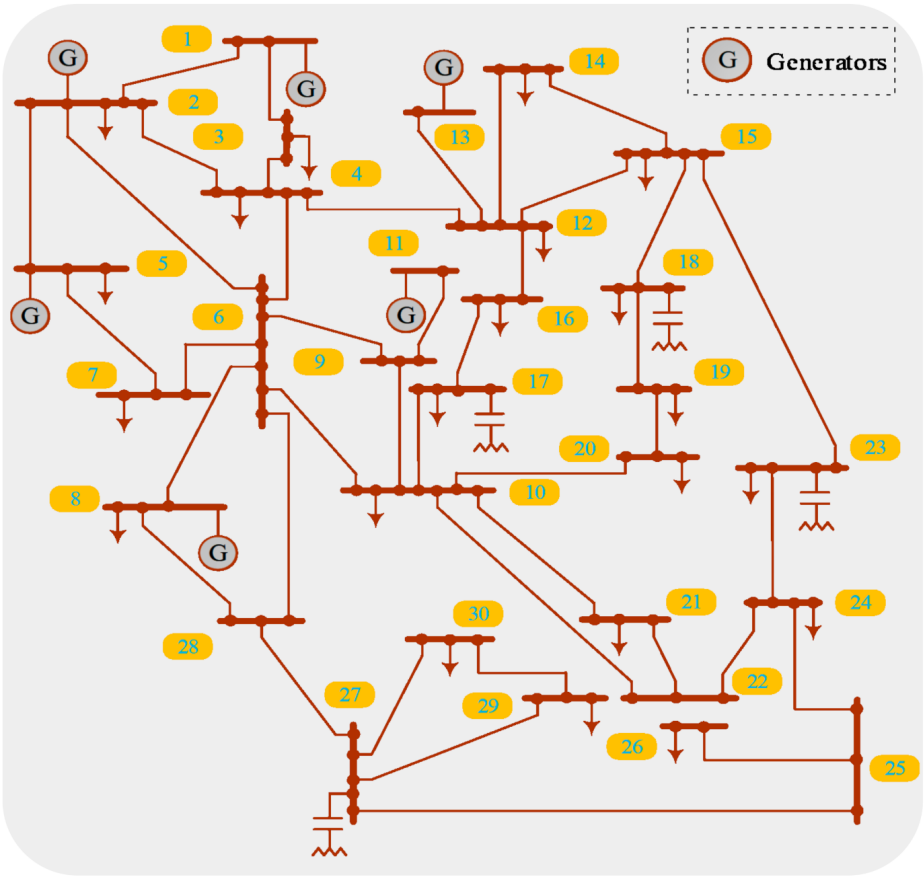


Figure 4. The IEEE 30-bus electrical network.

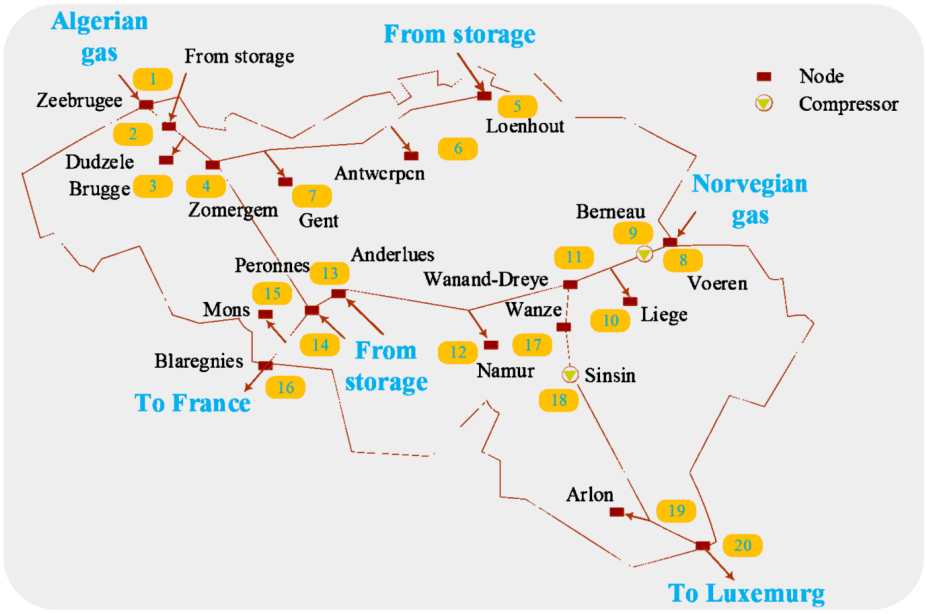


Figure 5. The 20-node natural gas network.

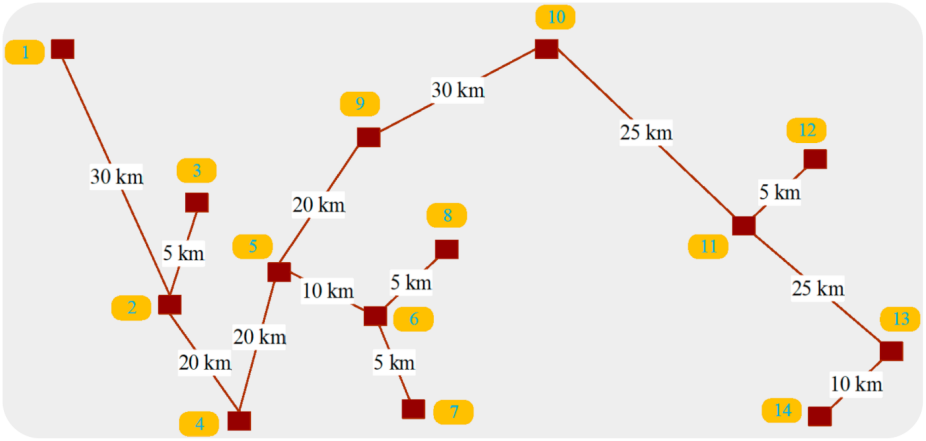


Figure 6. The 14-node district heating network.

Table 2. The data required for the networks.

Electrical Network	Natural Gas Network	District Heating Network
$a^{GC} = 0.01$ $b^{GC} = 4.0$ $c^{GC} = 150$	$GHV = 40.611$ $\eta^{GC} = 0.8$ $\alpha^{GC} = \gamma^{GC} = 0$ $\beta^{GC} = 0.001$ $\varepsilon_G = 0.05$ mm $z_G = 0.8$ $\delta_G = 0.6106$ $\lambda_G = 1.309$ $T_{0G} = 273.15$ $T_{GC} = 281.15$ $\pi_{0G} = 1.01325$ $\mu_G = 0.288 \times 10^{-6}$	$c_p = 4182$ $U_H = 0.2$ $\rho_W = 960$ $g = 9.81$ $\varepsilon_H = 1.25$ $\mu_W = 0.294 \times 10^{-6}$ $H_p = 100$ $\eta_{HP} = 0.65$ $T_g = 10\ ^\circ$C

Table 3. Connections Between Equipment and Subnets.

Unit	Electric Bus	Gas Node	Thermal Node
Slack generator	**1**	**12**	—
Generator 2	**2**	**19**	—
Compressor motor 1	**4**	**9**	—
CHP, boiler, and pump	**6**	**15**	**4**
CHP, boiler, and pump	**13**	**7**	**9**
CHP, boiler, and pump	**14**	**6**	**10**
CHP, boiler, and pump	**8**	**10**	**13**

The electrical network has two generators, three condensers, and 20 lines. In the simulation, each of these 25 items goes out of the circuit in sequence, and calculations are performed in the absence of the equipment. Security indicators are obtained in such conditions. By comparing the security indicators obtained in this situation, we can comment on the electrical network. It should be noted that in the electrical network, in one of the cases related to the outage of lines, part of the network becomes an island. In this application, the standard NR technique is utilized to solve the system equations, which is described completely in [18].

4.2. Results and Discussion

4.2.1. Test-System1: (IEEE 14-Bus)

The values obtained for security indicators in the electrical network are given in Figure 7. In Figure 7, the first five events are related to the outage of generator and condenser units, while another 20 events are obtained from the outage of the lines. The values obtained in the bar charts are indicators for PIV and the PIP through the lines. When these values are larger, the outage conditions of the unit or the corresponding line becomes more sensitive. Based on the results, the highest values for the indicators introduced occurred at the outage of line 10, where this line is between buses 5 and 6. According to Figure 7, the outage of the above line creates a significant effect on the network, which is also confirmed by the obtained indicators.

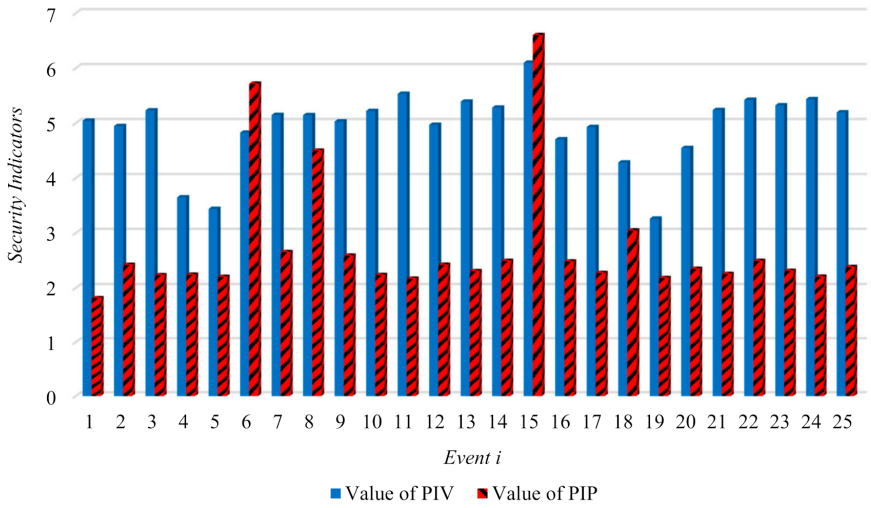


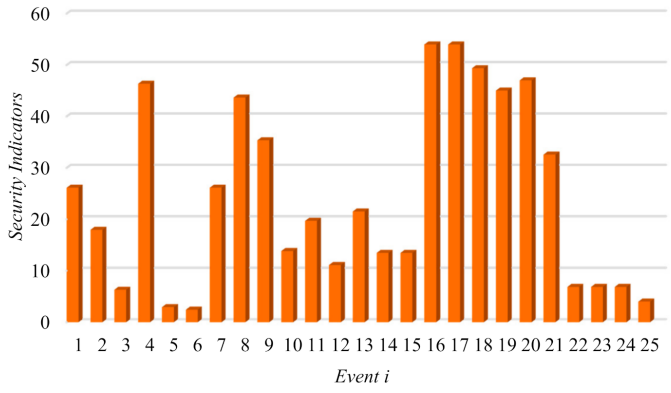
Figure 7. Security indicators of the electrical network corresponding to test-system 1.

There are nine heat supply sources and 13 heat lines in the district heating network. In this network, five boilers and four CHPs are installed, which are responsible for supplying heat to the loads. With the departure of each of these nine equipment or lines related to the network, the ENS coefficient is calculated. By comparing them, the most effective lines can be identified so that the security of the network can be provided to an acceptable

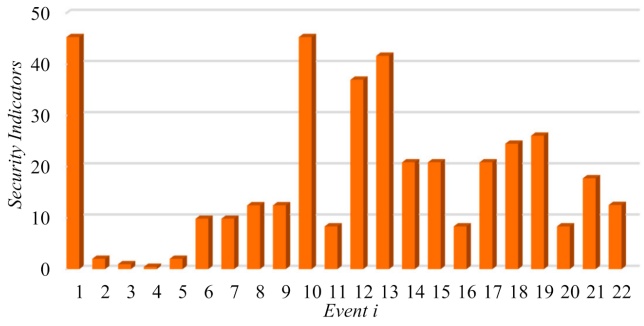
level. Obviously, due to the radial structure of the thermal network, the output of each line divides the network into two separate parts. Network security requires that production units in each of the sub-sectors are able to meet the needs of consumers. Therefore, if the amount of production in a part is higher than the amount of consumption, in such circumstances, all the needs of the network will be met in that part. Otherwise, part of the load will be unsecured, which is given in the ENS coefficient.

Similar to thermal networks, in the natural gas network, the goal is to remove gas lines and tanks, which will be used to obtain the ENS coefficient for the network. There are six gas tanks and 19 pipelines in the natural gas network. Gas networks also have a radial structure and when a line leaves them, the network is divided into two separate parts. Similar to the above, to supply all consumers in the event of an outage of units or lines, the amount of gas tank production must be higher than the amount consumed in that sector.

The curves of ENS corresponding to the natural gas and thermal networks are illustrated in Figure 8a,b, respectively. In Figure 8, the values of the first events are related to the output of the units and the output of the lines is given after that. For example, in the ENS of the natural gas network, the first six events are related to the outage of gas tanks, while the next 19 numbers are related to the outage of lines. The highest value obtained for the gas network is related to the outage of lines 10 and 11, which led to the value of 54.0026 for the security index. In the district heating network, the first nine values are related to the outage of heat production units, and the next 13 numbers are for the outage of lines. In the thermal network, the highest value obtained for ENS is related to the slack boiler, which is equal to 45.3125. In other words, the outage of the slack boiler has led to the highest ENS value.



(a)



(b)

Figure 8. The graphs of the ENS (Energy not supplied) index corresponding to test-system 1 for (**a**) natural gas, and (**b**) thermal networks.

One of the standard tools for evaluating the performance of integrated systems is sensitivity analysis. In this section, the sensitivity of security indicators to the amount of electrical network load is examined. Therefore, in Figures 9 and 10, the sensitivity of security indicators (PIV and PIP) from 80 to 120% loading is plotted.

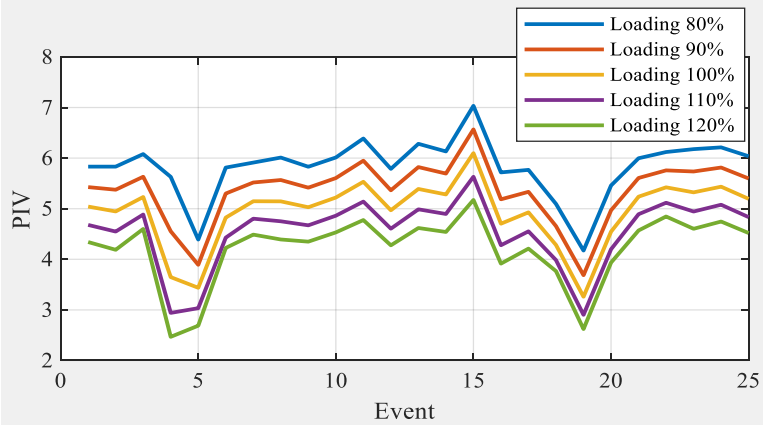


Figure 9. Sensitivity of the PIV (Performance index of voltage) index to load changes.

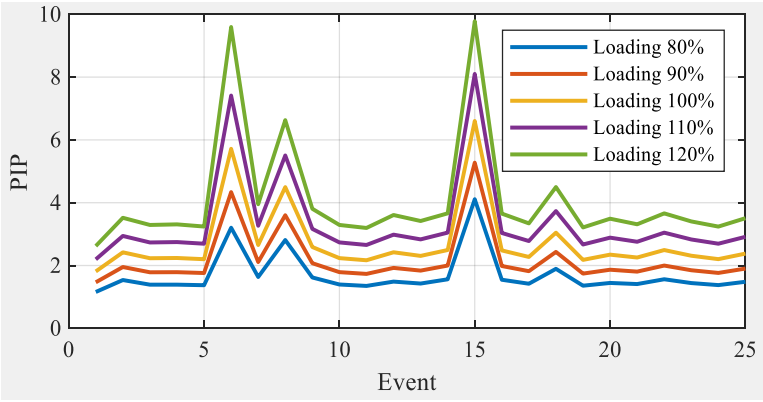


Figure 10. Sensitivity of PIP (Performance index of power) index to load changes.

By comparing Figures 11 and 12, it can be observed that, for example, 80% load has the highest PIP value and the lowest PIV value, while for 120% loading, the opposite happened. In terms of voltage profile, the voltage sensitivity of electrical network buses can also be obtained by the amount of load, where this problem is illustrated in Figure 11.

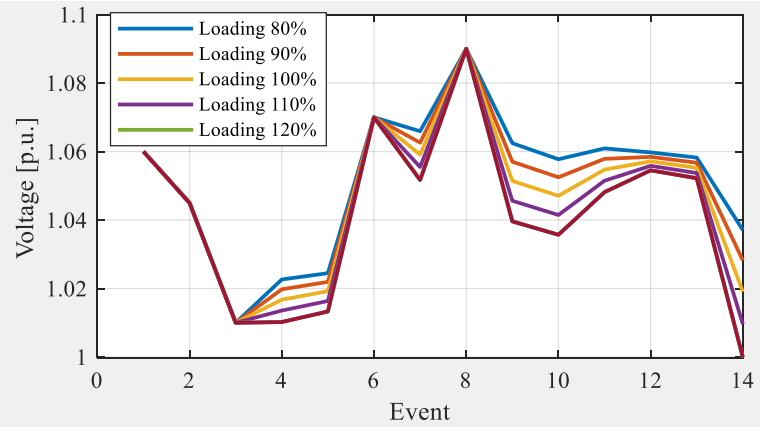


Figure 11. The sensitivity of electrical network voltage to load changes.

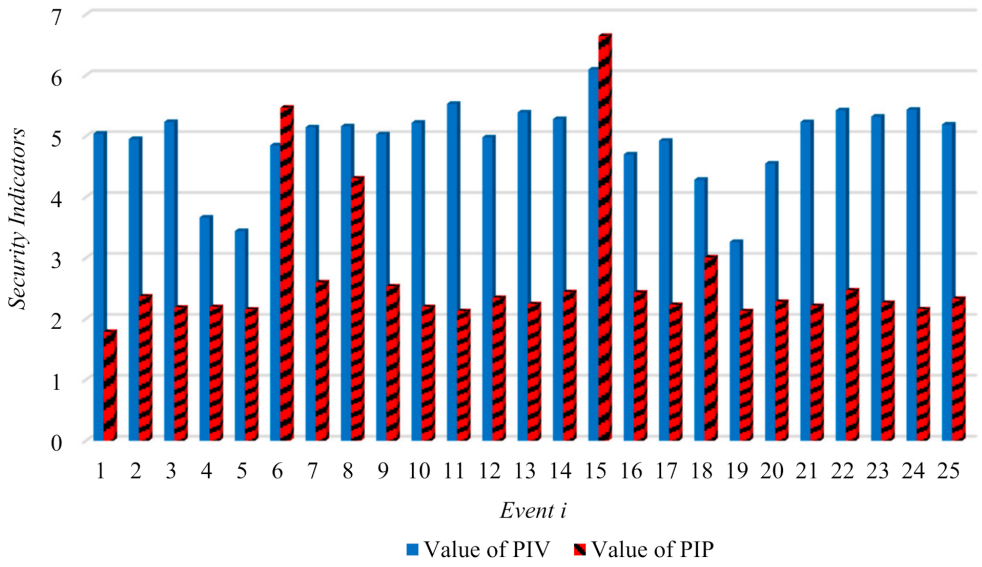


Figure 12. Security indicators for the electrical network of test-system 1 in scenario 75.

Sometimes security indicators can be examined in the probabilistic space. In this way, it first considers the network loads as probabilities, and then repeats them in 100 simulation scenarios using the Monte Carlo method. In this section, the results of scenarios 75 and 100 are given, for example, in Figures 12 and 13.

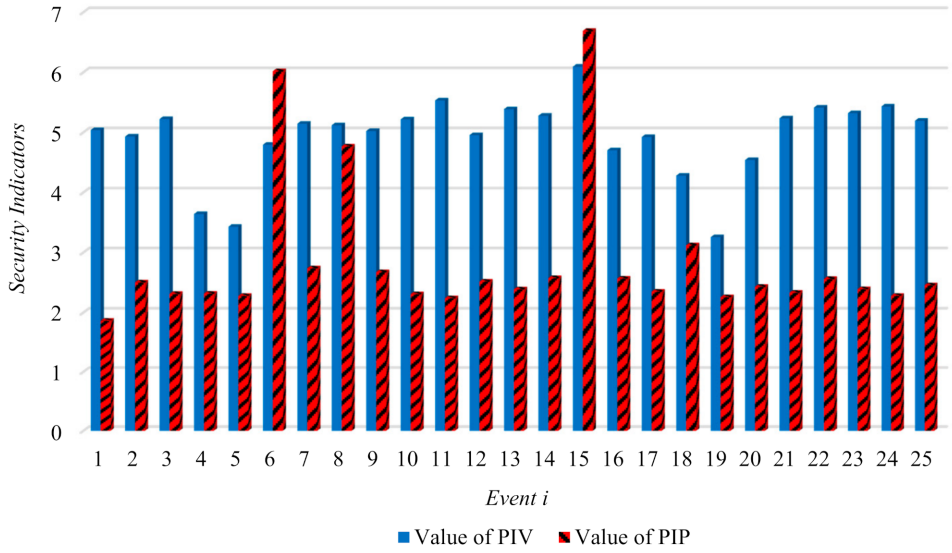
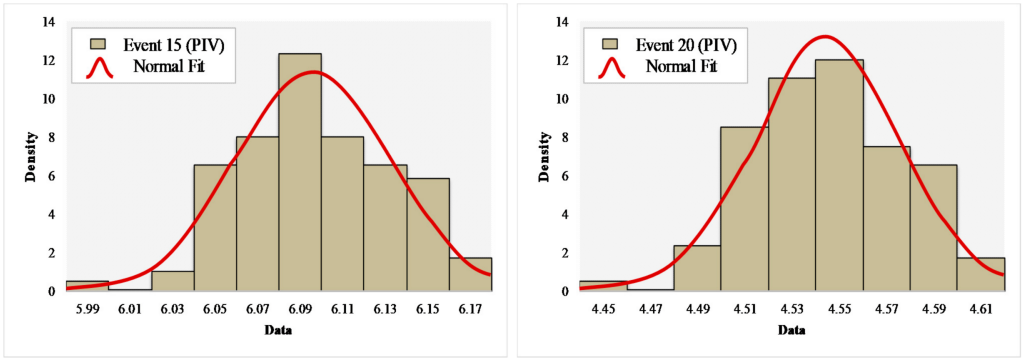


Figure 13. Security indicators for the electrical network of test-system 1 in scenario 100.

The critical observation of Figures 12 and 13 reveals which of the highest values obtained for PIV and PIP at both the scenarios (scenario 75 and scenario 100) is related to the event 15^{the}. In scenario 75, the event 15^{the} is as 6.0950 for PIV and 6.6478 for PIP, while it is obtained as 6.0942 for PIV and 6.6901 for PIP in scenario 100. Thus, it can be inferred that among the 25 events, the worst condition is imposed on the network by this event 15^{the}.

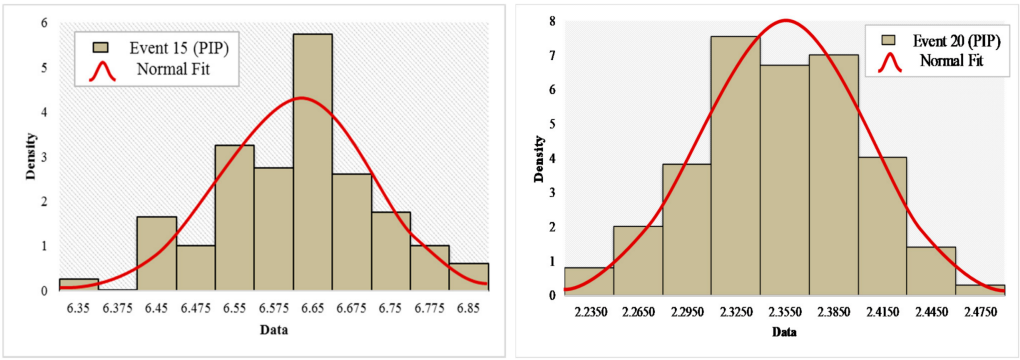
In the natural gas and district heating networks, these values are kept constant due to no-load distribution. While they can be changed if needed. To better express the potential problem, events 15 and 20 are obtained from the security indicators of PIV and PIP which

are illustrated in Figures 14 and 15, respectively. These figures demonstrate the probability of each outage where the shapes are approximated by a normal curve.



(**a**) (**b**)

Figure 14. The probability distribution of the PIV index for test-system 1 corresponding to (**a**) the 15th event, and (**b**) the 20th event.



(**a**) (**b**)

Figure 15. The probability distribution of the PIP index for test-system 1 corresponding to (**a**) the 15th event, and (**b**) the 20th event.

In Figures 14 and 15, based on the normal distribution functions, 100 random samples are selected for the electrical network loads. For each of the outages in the electrical network, the values of PIP and PIV are obtained for all these possible samples. The 15th event experienced higher values in comparison with the 20th event, which confirms that the worst condition of supply is imposed on the network by the 15th event, as demonstrated in the previous analysis.

4.2.2. Test-System 2: (IEEE 30-Bus)

The 30-bus electrical network has 6 generators and 41 transmission lines. Similar to the previous case test, in the simulation of each of the above 47 cases, the circuit of elements are cut off and calculations are performed in the absence of the element. As an example, the values obtained for security indicators at a specific load (network outage load) for the electrical network are given in Figure 16. In this Figure, the first six lines related to the outage of generator units and another 41 lines related to the outage of lines are obtained. According to the results, the highest value for the PIV index occurred at the outage of the third generator, and the highest value for the PIP occurred at the outage of the 30th line.

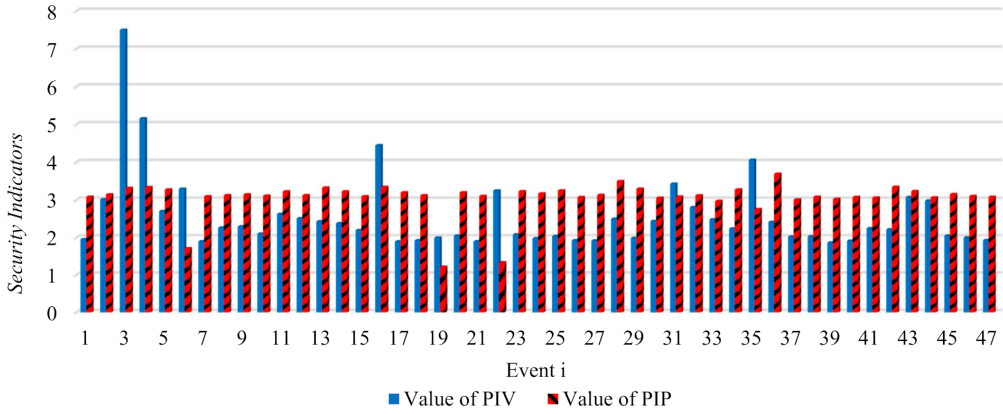
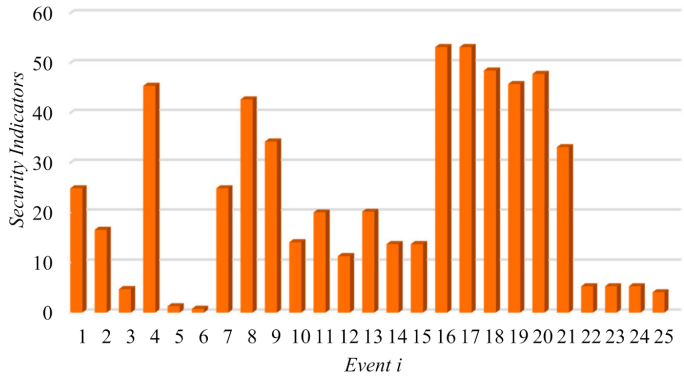
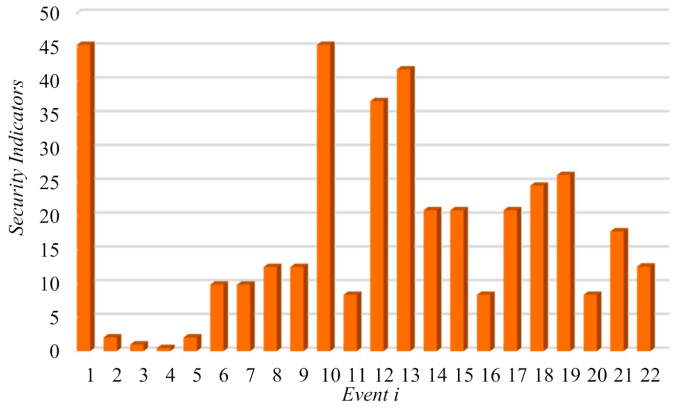


Figure 16. Security indicators of the electrical network corresponding to test-system 2.

Figure 17 shows the ENS values of gas and thermal networks. It is observed that due to the different amount of fuel consumption of the units related to the 30-bus network, the values obtained in this test-system are different compared to the corresponding case in the first test-system (IEEE 14-bus).



(**a**)



(**b**)

Figure 17. The graphs of the ENS index corresponding to test-system 2 for (**a**) natural gas and (**b**) thermal networks.

In order to analyze the sensitivity indices in the probabilistic way, the network loads are considered as probabilistic, and implemented in 100 scenarios by Monte Carlo method. In this section, for example, the results of scenario 75 are illustrated in Figure 18. Possible behavior related to event 20 is obtained from the security indicators, as depicted in Figure 19.

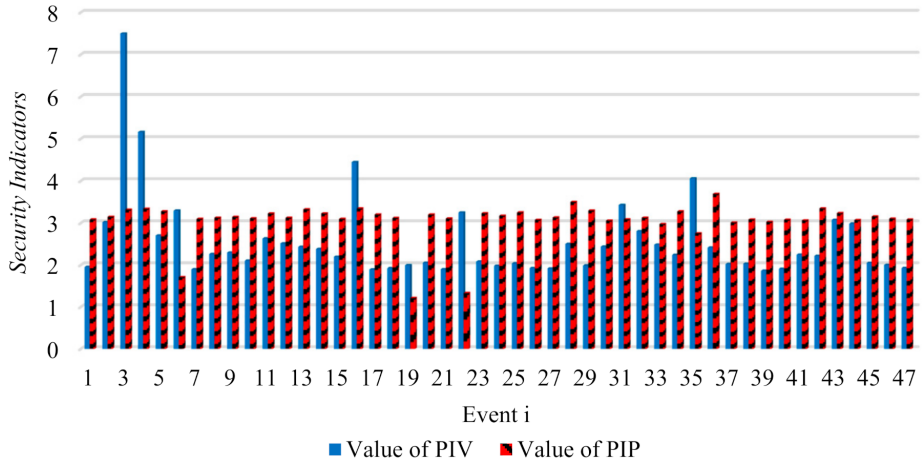
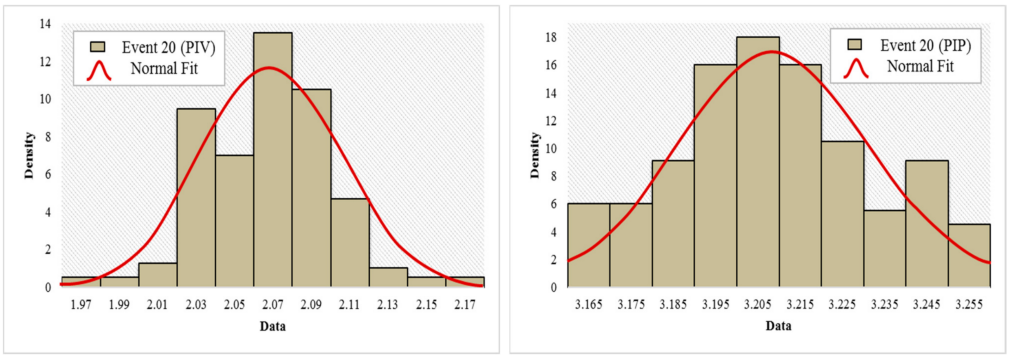


Figure 18. Security indicators for the electrical network of test-system 2 in scenario 75.



(**a**) (**b**)

Figure 19. The probability distribution corresponding to the 20th event for test-system 2: (**a**) the PIV index, and (**b**) the PIP index.

5. Conclusions

The MCESs consisting of electrical, natural gas, and thermal networks have always been of interest to operators. One of the most important studies related to such networks is the study of a security problem concerning its components and energy carriers. This paper examined security with indicators appropriate to each network, including PIP/PIV for electrical networks and the ENS index for natural gas and thermal networks. Firstly, the safe operation of an electrical network for an IEEE 14-bus was investigated, and the critical security indicators in the network (PIV and PIP) from 80 to 120% loading were analyzed and compared. For a comprehensive study of MCES security analysis, the ENS of natural gas and district heating networks was assessed. By implementing the Monte Carlo technique with 100 simulation repetitions, security indicators were evaluated using the probabilistic method. In addition, the probability distribution corresponding to the PIP and PIV for the 15^{the} and 20^{the} events were analyzed. The simulation outcomes confirm that the proposed method is suitable for checking the security of subnets. To study the feasibilities of the suggested approach, the study is extended to a more complex plant, entitled the IEEE 30-bus system. The results show that by changing the case study and

the networks under study, the proposed method is still effective and not dependent on the problem conditions. In addition, the proposed method is not dependent on the system elements and their number, and can be adopted for any number of equipment installed in the subnets.

Author Contributions: Formal analysis, T.N.; Investigation, J.E.; Resources, M.S. All authors have read and agreed to the published version of the manuscript.

Funding: This research received no external funding.

Institutional Review Board Statement: Not applicable.

Informed Consent Statement: Not applicable.

Data Availability Statement: The data presented in this study are available on request from the corresponding author.

Conflicts of Interest: The authors declare no conflict of interest.

Abbreviations

A. *MCES Coefficients/Variables*	
V_i, V_j	Voltage amplitude of buses i and j
Y_{ij}	Admittance between buses i and j
$P_{E,i}^{dem}$, $Q_{E,i}^{dem}$	Active and reactive demand of the i^{the} bus
θ_i, θ_j	Voltage angle of buses i and j
θ_{ij}	Difference between angles of buses i and bus j
$G_{E,ij}^{line}$, $B_{E,ij}^{line}$	Conductance and sustenance of transmission line between buses i and j
$f_{G,ij}^{line}$	Gas flow passing through the pipeline connected between nodes i and j
$f_{G,i}^{dem}$, $C_{G,ij}^{line}$	Gas demand and constant of the pipeline connected between nodes i and j
δ_G	Gas density against air
ε_G	Specific gravity of the gas
Z_G	Average coefficient of gas compressibility
λ_G, T_G	Specific heat ratio and gas temperature
$L_{G,ij}^{line}$, $D_{G,ij}^{line}$	Length and diameter of the gas pipeline between nodes i and j
$P_{r,i}$, $P_{r,j}$	Gas pressures related to nodes i and j
P_{r0}, T_0	Standard values of pressure and temperature
$\dot{m}$	Mass flow rate of through pipelines
T_{si}, T_{ri}	Supply and return temperature at node i
c_p	Water specific heat capacity
$\psi_{H,ij}^{line}$	Transmission pipe constant
T_g	Ambient temperature
U	Heat transfer coefficient of the pipe length
$L_{H,ij}^{line}$, $\dot{m}_{H,ij}^{line}$	Length and mass flow rate between nodes i and j
a_i^{gen}, b_i^{gen}, c_i^{gen}	Cost coefficient of the i^{th} generator
$P_{E,i}^{gen}$	Generated power by i^{th} generator
HR_i^{gen}	Heat rate of the i^{th} generator
GHV_G	Gross heating value
$P_{E,i}^{chp}$, $Q_{H,i}^{chp}$	Electrical and heat power of i^{th} CHP
$Q_{H,i}^{chp,min}$, $Q_{H,i}^{chp,max}$	Minimum/maximum amount of heat output
$T_{s,i}^{chp}$	Supply temperature of i^{th} CHP
$y_{1,i}^{chp}$, $y_{2,i}^{chp}$	Load effect variables
$\eta_{t,i}^{chp}$	Thermal efficiency of the i^{th} CHP
$Q_{H,i}^{boil}$	Heat power of the i^{th} boiler
a_i^{boil}, b_i^{boil}	Part load constants of the i^{th} boiler
$Pr_{i,in}^{comp}$, $Pr_{i,out}^{comp}$	Inlet and outlet pressures of i^{th} compressor

η_{ij}^{comp}	Compressor efficiency
$\dot{m}_H^{pump}$	Mass flow rate through the pump
H^{pump}	Pump head
g	Ground gravity
η_i^{pump}	Efficiency of the i^{th} circulating pump
B. *Security Assessment Coefficients/Variables*	
P_l	Power passing through the line l
P_l^{Max}	Maximum apparent power passing through line l
NL	Number of lines in the power system
w_l	Positive weight coefficient of network lines
n	Constant parameter
w_{vi}	Weight factor for the bus i
V_i^{min},V_i^{Max}	Minimum/maximum acceptable voltages on the bus i
fif_i,QIQ_i	Amount of gas and thermal ENS in the event i
Abbreviations	
MCES	Multi-carrier energy system
OPF	Optimal power flow
CHP	Combined heat and power
ENS	Energy not supplied
HR	Heat rate
GHV	Gross heating value
MC	Monte Carlo
PIP	Power performance index
PIV	Voltage performance index

References

1. Arabkoohsar, A.; Nami, H. Thermodynamic and economic analyses of a hybrid waste-driven CHP–ORC plant with exhaust heat recovery. *Energy Convers. Manag.* **2019**, *187*, 512–522. [CrossRef]
2. Diesendorf, M.; Elliston, B. The feasibility of 100% renewable electricity systems: A response to critics. *Renew. Sustain. Energy Rev.* **2018**, *93*, 318–330. [CrossRef]
3. Arabkoohsar, A.; Andresen, G. Supporting district heating and cooling networks with a bifunctional solar assisted absorption chiller. *Energy Convers. Manag.* **2017**, *148*, 184–196. [CrossRef]
4. Nazari-Heris, M.; Mohammadi-Ivatloo, B.; Asadi, S. Optimal Operation of Multi-Carrier Energy Networks Considering Uncertain Parameters and Thermal Energy Storage. *Sustainability* **2020**, *12*, 5158. [CrossRef]
5. Martinez-Mares, A.; Fuerte-Esquivel, C.R. A Unified Gas and Power Flow Analysis in Natural Gas and Electricity Coupled Networks. *IEEE Trans. Power Syst.* **2012**, *27*, 2156–2166. [CrossRef]
6. Geidl, M.; Andersson, G. Operational and structural optimization of multi-carrier energy systems. *Eur. Trans. Electr. Power* **2006**, *16*, 463–477. [CrossRef]
7. Nazari-Heris, M.; Mohammadi-Ivatloo, B.; Asadi, S. Optimal operation of multi-carrier energy networks with gas, power, heating, and water energy sources considering different energy storage technologies. *J. Energy Storage* **2020**, *31*, 101574. [CrossRef]
8. Geidl, M.; Andersson, G. Operational and topological optimization of multi-carrier energy systems. In Proceedings of the International Conference on Future Power Systems, Amsterdam, The Netherlands, 16–18 November 2005; p. 6.
9. Geidl, M.; Andersson, G. Optimal Power Flow of Multiple Energy Carriers. *IEEE Trans. Power Syst.* **2007**, *22*, 145–155. [CrossRef]
10. Waller-Hunter, J. *Caring for Climate: A Guide to the Climate Change Convention and the Kyoto Protocol*; UNFCCC: Bonn, France, 2005.
11. Heris, M.-N.; Mirzaei, M.A.; Asadi, S.; Mohammadi-Ivatloo, B.; Zare, K.; Jebelli, H.; Marzband, M. Evaluation of hydrogen storage technology in risk-constrained stochastic scheduling of multi-carrier energy systems considering power, gas and heating network constraints. *Int. J. Hydrogen Energy* **2020**, *45*, 30129–30141. [CrossRef]
12. Niemi, R.; Mikkola, J.; Lund, P. Urban energy systems with smart multi-carrier energy networks and renewable energy generation. *Renew. Energy* **2012**, *48*, 524–536. [CrossRef]
13. Geidl, M. Integrated Modeling and Optimization of Multi-Carrier Energy Systems. Ph.D. Thesis, Technical University ETH Zurich, Zurich, Switzerland, 2007.
14. Arnold, M.; Andersson, G. Decomposed Electricity and Natural Gas Optimal Power Flow. Available online: https://citeseerx.ist.psu.edu/viewdoc/download?doi=10.1.1.164.5769&rep=rep1&type=pdf (accessed on 1 January 2021).
15. Moeini-Aghtaie, M.; Abbaspour, A.; Fotuhi-Firuzabad, M.; Hajipour, E. A Decomposed Solution to Multiple-Energy Carriers Optimal Power Flow. *IEEE Trans. Power Syst.* **2013**, *29*, 707–716. [CrossRef]

16. Li, Q.; An, S.; Gedra, T.W. Solving Natural Gas Loadflow Problems Using Electric Loadflow Techniques. pp. 1–7. Available online: https://citeseerx.ist.psu.edu/viewdoc/download?doi=10.1.1.80.9709&rep=rep1&type=pdf (accessed on 28 February 2021).
17. Li, X.; Tian, G.; Shi, Q.; Jiang, T.; Li, F.; Jia, H. Security region of natural gas network in electricity-gas integrated energy system. *Int. J. Electr. Power Energy Syst.* **2020**, *117*, 105601. [CrossRef]
18. Shabanpour-Haghighi, A.; Seifi, A.R. An Integrated Steady-State Operation Assessment of Electrical, Natural Gas, and District Heating Networks. *IEEE Trans. Power Syst.* **2015**, *31*, 3636–3647. [CrossRef]
19. Gargari, M.Z.; Ghaffarpour, R. Reliability evaluation of multi-carrier energy system with different level of demands under various weather situation. *Energy* **2020**, *196*, 117091. [CrossRef]
20. Bai, L.; Li, F.; Jiang, T.; Jia, H. Robust Scheduling for Wind Integrated Energy Systems Considering Gas Pipeline and Power Transmission N-1 Contingencies. *IEEE Trans. Power Syst.* **2016**, *32*, 1. [CrossRef]
21. Chen, S.; Wei, Z.; Sun, G.; Sun, Y.; Lu, N. Steady-state security regions of electricity-gas integrated energy systems. In Proceedings of the IEEE Power and Energy Society General Meeting (PESGM), Boston, MA, USA, 17–21 July 2016; pp. 1–5.
22. Li, G.; Kou, Y.; Jiang, J.; Lin, Y.; Bie, Z. Researches on the reliability evaluation of integrated energy system based on Energy Hub. In Proceedings of the China International Conference on Electricity Distribution (CICED), Xi'an, China, 10–13 August 2016; pp. 1–9.
23. Yang, H.; Zhang, Y.; Ma, Y.; Zhang, D.; Sun, L.; Xia, S. Reliability assessment of integrated energy system considering the uncertainty of natural gas pipeline network system. *IET Gener. Transm. Distrib.* **2019**, *13*, 5033–5041. [CrossRef]
24. Li, G.; Zhang, R.; Jiang, T.; Chen, H.; Bai, L.; Li, X. Security-constrained bi-level economic dispatch model for integrated natural gas and electricity systems considering wind power and power-to-gas process. *Appl. Energy* **2017**, *194*, 696–704. [CrossRef]
25. Azzuni, A.; Breyer, C. Energy security and energy storage technologies. *Energy Procedia* **2018**, *155*, 237–258. [CrossRef]
26. Li, T.; Eremia, M.; Shahidehpour, M. Interdependency of Natural Gas Network and Power System Security. *IEEE Trans. Power Syst.* **2008**, *23*, 1817–1824. [CrossRef]
27. Yan, M.; Zhang, N.; Ai, X.; Shahidehpour, M.; Kang, C.; Wen, J. Robust two-stage regional-district scheduling of multi-carrier energy systems with a large penetration of wind power. *IEEE Trans. Sustain. Energy* **2018**, *10*, 1227–1239. [CrossRef]
28. Shariatkhah, M.-H.; Haghifam, M.-R.; Parsa-Moghaddam, M.; Siano, P. Modeling the reliability of multi-carrier energy systems considering dynamic behavior of thermal loads. *Energy Build.* **2015**, *103*, 375–383. [CrossRef]
29. Fathtabar, H.; Barforoushi, T.; Shahabi, M. Dynamic long-term expansion planning of generation resources and electric transmission network in multi-carrier energy systems. *Int. J. Electr. Power Energy Syst.* **2018**, *102*, 97–109. [CrossRef]
30. Naik, S.; Khedkar, M.; Bhat, S. Effect of line contingency on static voltage stability and maximum loadability in large multi bus power system. *Int. J. Electr. Power Energy Syst.* **2015**, *67*, 448–452. [CrossRef]
31. Pazouki, S.; Mohsenzadeh, A.; Ardalan, S.; Haghifam, M. Optimal place, size, and operation of combined heat and power in multi carrier energy networks considering network reliability, power loss, and voltage profile. *IET Gener. Transm. Distrib.* **2016**, *10*, 1615–1621. [CrossRef]
32. Lei, Y.; Hou, K.; Wang, Y.; Jia, H.; Zhang, P.; Mu, Y.; Jin, X.; Sui, B. A new reliability assessment approach for integrated energy systems: Using hierarchical decoupling optimization framework and impact-increment based state enumeration method. *Appl. Energy* **2018**, *210*, 1237–1250. [CrossRef]
33. Liu, X.; Jenkins, N.; Wu, J.; Bagdanavicius, A. Combined Analysis of Electricity and Heat Networks. *Energy Procedia* **2014**, *61*, 155–159. [CrossRef]
34. Shabanpour-Haghighi, A.; Seifi, A.R. Simultaneous integrated optimal energy flow of electricity, gas, and heat. *Energy Convers. Manag.* **2015**, *101*, 579–591. [CrossRef]
35. Liu, X.; Wu, J.; Jenkins, N.; Bagdanavicius, A. Combined analysis of electricity and heat networks. *Appl. Energy* **2016**, *162*, 1238–1250. [CrossRef]
36. Shabanpour-Haghighi, A.; Seifi, A.R. Energy Flow Optimization in Multicarrier Systems. *IEEE Trans. Ind. Inform.* **2015**, *11*, 1067–1077. [CrossRef]
37. Sachan, S.; Gupta, C. Analysis of contingent conditions in power system. In Proceedings of the 2014 Students Conference on Engineering and Systems, Allahabad, India, 28–30 May 2014; pp. 1–5.
38. Sekhar, P.; Mohanty, S. Power system contingency ranking using Newton Raphson load flow method. In Proceedings of the Annual IEEE India Conference (INDICON), Mumbay, India, 13–15 December 2013; pp. 1–4.
39. Gongada, S.R.; Rao, T.S.; Rao, P.M.; Salima, S. Power system contingency ranking using fast decoupled load flow method. In Proceedings of the International Conference on Electrical, Electronics and Optimization Techniques (ICEEOT), Chennai, India, 3–5 March 2016; pp. 4373–4376.
40. Hashemi-Dezaki, H.; Askarian-Abyaneh, H.; Haeri-Khiavi, H. Reliability optimization of electrical distribution systems using internal loops to minimize energy not-supplied (ENS). *J. Appl. Res. Technol.* **2015**, *13*, 416–424. [CrossRef]
41. Heggset, J.; Kjolle, G.H.; Trengereid, F.; Ween, H.O. Quality of supply in the deregulated Norwegian power system. In Proceedings of the IEEE Porto Power Techology Proceedings (Cat. No.01EX502), Porto, Portugal, 10–13 September 2001.
42. Unsihuay, C.; Lima, J.W.M.; De Souza, A.Z. Modeling the Integrated Natural Gas and Electricity Optimal Power Flow. In Proceedings of the IEEE Power Engineering Society General Meeting, Tampa, FL, USA, 24–28 June 2007; pp. 1–7.

43. Soeprijanto, A.; Abdillah, M. Type 2 fuzzy adaptive binary particle swarm optimization for optimal placement and sizing of distributed generation. In Proceedings of the 2nd International Conference on Instrumentation Communications, Information Technology, and Biomedical Engineering, Bandung, Indonesia, 8–9 November 2011; pp. 233–238.
44. Iyambo, P.; Tzoneva, R. Transient stability analysis of the IEEE 14-bus electric power system. In Proceedings of the 2nd International Conference on Instrumentation, Communications, Information Technology and Biomedical Engineering, Bandung, Indonesia, 8–9 November 2011; pp. 1–9.
45. De Wolf, D.; Smeers, Y. The Gas Transmission Problem Solved by an Extension of the Simplex Algorithm. *Manag. Sci.* **2000**, *46*, 1454–1465. [CrossRef]